Phase transitions driven by magnetoelectric and interfacial Dzyaloshinskii-Moriya interaction

Ildus F Sharafullin, Alina R Yuldasheva, Danil I Abdrakhmanov, Ilgiz R Kizirgulov, Hung T Diep

PHASE TRANSITIONS DRIVEN BY MAGNETOELECTRIC AND INTERFACIAL DZYALOSHINSKII-MORIYA INTERACTION

Ildus F. Sharafullin [a*], Alina R. Yuldasheva [a], Danil I. Abdrachmanov [a],

Ilgiz R. Kizirgulov [a], Hung T. Diep [b]

[a] *Institute of Physics and Technology, Ufa University of Science and Technologies, 32, Validy str, 450076, Ufa, Russia.*

[b] *Laboratoire de Physique Théorique et Modélisation, CY Cergy Paris Université CNRS, UMR 8089, 2 Avenue Adolphe Chauvin, 95302 Cergy-Pontoise, France.*

** Corresponding author. E-mail address: sharafullinif@yandex.ru*

Abstract

In this paper, we study phase transitions in a magnetoelectric bilayer with two order parameters using Monte Carlo simulation. We investigate the effects of temperature, magnetoelectric coupling, and anisotropy in the multiferroic bilayer formed by a frustrated antiferromagnetic layer with Heisenberg spins and a triangular lattice ferroelectric layer. We show that magnetic frustration induces creation of skyrmions and a skyrmion lattice at moderate values of Dzyaloshinskii-Moriya interaction and interface magnetoelectric coupling with adjacent ferroelectric layer. The skyrmion crystal is stable up to relatively high temperatures. The effect of anisotropy is to cause only a shift of the critical temperature without changing the type of the phase transition. The phase of the skyrmion lattice becomes more resistant and stable to temperature fluctuations in the case of a highly anisotropic frustrated film.

Keywords: phase transition, bilayer, skyrmion, skyrmion lattice, Monte Carlo simulation, magnetoelectric interaction

1. INTRODUCTION

In the last few decades, nonuniform spin structures, such as skyrmions in nanofilms with magnetic or ferroelectric long-range ordering or systems with both types of ordering has become a central focus of condensed matter physics [1-11]. Although skyrmions were invented for the stablization of vortex configurations in the field theory, it allows for a number of generalizations, such as ferroelectric skyrmions [12] and magnetic skyrmions. Magnetic skyrmion is a topologically nontrivial local

spin texture that forms at low temperature (in special cases at zero temperature) from competition among exchange interactions, exchange frustrations and external fields.

On the one hand, skyrmions can be used to store, transmit, and manipulate information with high efficiency in terms of energy consumption due to their topologically protected textures [13-16]. On the other hand, magnetic skyrmions form lattices in antiferromagnetic, synthetic antiferromagnetic and compensated ferrimagnetic materials – it represents an exciting state of matter[17-18]. Experimentally, there is ample of evidence that thermodynamically stable skyrmion lattice phases occupy a wide region in the phase diagrams of many materials, most notably the thin films and superlattices [19-22]. They were observed [20,21] in several multiferroics, crystals (and epitaxial films) with certain symmetry [23]**.** For thin films with ferromagnetic long –range ordering skyrmions usually appear only as result a competition of exchange and Dzyaloshinskii – Moriya interactions in the presence of magnetic field.

Due to the magnetoelectric coupling effect of multiferroic materials, magnetoelectric interaction is an important force to modulate skyrmions. Recently, many works have been done on the mechanical control of skyrmions. For example, Wang et al. [24] have found that the ferroelectric proximity effect at the interface of heterostructure BaTiO3/SrRuO3 triggers a sizeable Dzyaloshinskii–Moriya interaction, thus stabilizing robust skyrmions. Legrand et al. [25] have successfully demonstrated that room-temperature antiferromagnetic skyrmions can be stabilized in synthetic antiferromagnets (SAFs). Shibata et al. [26] have observed very large anisotropic deformations of skyrmions induced by uniaxial strains, which indicates a large strain-induced anisotropy in DMI. Koretsune et al. [27] have demonstrated that the value of DMI coefficient, which controls the stability and size of skyrmions, can be controlled as a function of the external strain. Wang et al. [28] have explored the uniaxial strain modulation of topological phase transition in ferromagnetic thin films by using a phase field model, in which the ferromagnetic-to-skyrmion and skyrmion-to-helical phase transitions take place sequentially as a uniaxial tensile strain increases

under specific magnetic fields. In the above-mentioned mechanical control of skyrmions, however, only a uniform strain or stress has been employed and thus an external magnetic field is needed to stabilize the skyrmions.

As already mentioned skyrmions are promising candidates for topological computation. Such binary and ternary memory device based on skyrmion (all-electric skyrmion-based devices, ultra-low dissipation devices) can be realized in different physical setups, such as ternary proccessor [29, 30]. The stability of topologically protected vortical spin textures can make the new memory devices based on skyrmions nonvolatile, and low energies for manipulation will reduce the cost of rewriting compared to current technologies.

Distinctly different from ferromagnetic materials, the mobile skyrmions in antiferromagnetic nanofilms move along the expected trajectory (along of the acting force i.e. the external field or current) [31, 32]. Comprehensive studies of skyrmions in antiferromagnetic materials are important from the point of view of future technical applications, because apart from the dynamic resistance of skyrmions to the Hall effect, the sufficiently large values Dzyaloshinskii-Moriya interaction (DMI) are more commonly found in antiferromagnetic (AFM) materials than ferromagnetic (FM) materials. We note that Mohylna et al. explored the emergence of skyrmion lattice in the absence of DMI in classical overfrustrated Heisenberg antiferromagnet on triangular lattice under external magnetic fields, the presence of the skyrmion phase in a frustrated triangular lattice antiferromagnet in the absence of the DMI was confirmed experimentally very recently [33,34]. On the roadmap of skyrmion-based modern hi-tech manufacturing, creation and stabilization of skyrmions are at the peak of necessity. In this article we show that magnetic frustration in the multiferroic bilayer system described by frustrated antiferromagnetic Heisenberg model on triangular lattice, induces creation of skyrmions and emergence of skyrmion lattice at moderate values of Dzyaloshinskii-Moriya interaction and interface magnetoelectric coupling with adjacent ferroelectric layer. Furthermore, we show that at zero magnetic field two kinds of exotic phases emerge according to the competition of different type interactions

between spins and polarizations. For this purpose we employ two complementary approaches: the steepest descent method to calculate the ground state spin configuration and to explore the phase diagram at $T = 0$, and Monte-Carlo (MC) simulations to incorporate thermal fluctuations and the effect of magnetoelectric coupling and anisotropy. The rest of the manuscript is organized as follows. In Sec. II we introduce the frustrated model of bilayer and present the $T = 0$ magnetic phase diagram at zero field. Then we discuss skyrmion lattice and distributed skyrmion states. In Sec. III we show our simulations analysis at finite temperature, identify phase transitions and the influence of anisotropy on critical temperature regions at zero external magnetic field. Section IV is devoted to the summary and conclusions.

2. MODEL SYSTEM AND SIMULATION METHODS

A. Model

Here we propose a model system which allows the existence of stable skyrmion lattice at moderate values of interface coupling and Dzyaloshinskii – Moriya interaction in the frustrated antiferromagnetic/ferroelectric ultrathin films, the model system is sketched in Fig. 1.

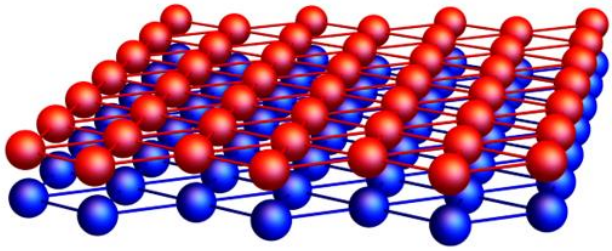

(a)

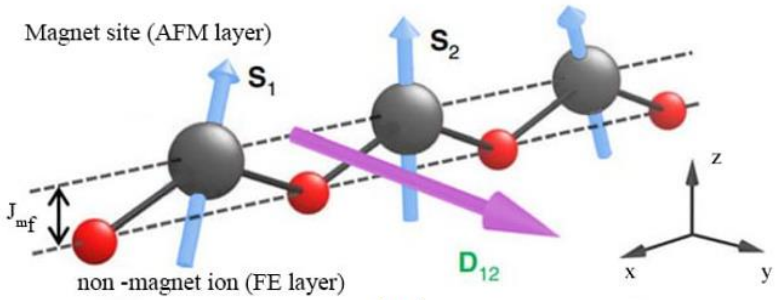

(b)

Fig. 1. (a) Magneto-ferroelectric bilayer; (b) positions of the spins in the xy plane and the position of the non-magnetic ion, defining the Dzyaloshinskii-Moriya (DM) vector.

Each layer has dimensions $L \times L$ in xy plane. We assume periodic boundary conditions in all directions, the lattice sites of the antiferromagnetic layer of this bilayer are occupied by interacting Heisenberg spins $\vec{S}$, while the lattice sites of the ferroelectric layer are occupied by interacting polarizations $\vec{P}$. The Hamiltonian of the system is defined as follows:

$$H_m = -\sum_{i,j} J_{i,j}^m \overrightarrow{S_\iota} \cdot \overrightarrow{S_J} - \sum_{i,j} J_{i,j}^f \overrightarrow{P_\iota} \cdot \overrightarrow{P_J} - \sum_{i,j} \vec{D}_{i,j} \cdot \left[\overrightarrow{S_\iota} \times \overrightarrow{S_J}\right] - K \sum_i \left(S_i^x S_{i+\hat{y}}^x + S_i^y S_{i+\hat{x}}^y\right) - H_{mf} \qquad (1)$$

We focus on the frustrated antiferromagnetic Heisenberg model on the triangular lattice which incorporates different levels of frustration in this lattice geometry. The first term here is the Hamiltonian of the antiferromagnetic subsystem, the second - of the ferroelectric subsystem, the third term is the DM interaction between NN spins in the frustrated antiferromagnetic layer, the following K term is the anisotropy interaction, and the last term is the Hamiltonian of their interlayer magnetoelectric interaction which is given below. We assume here $J_{i,j}^m < 0$ characterizes the antiferromagnetic interaction between one spin and its six in – plane nearest neighbors (NN). We consider it to be the same for all NN within a layer. $\overrightarrow{S_\iota}$ is the spin vector on the i-th site. $\overrightarrow{P_\iota}$ is the polarization z component at the i-th site assumed to have only two values ±1, $J_{i,j}^f > 0$ - the NN interaction, similar for all NN. Note that in the DM interaction energy between two spins S_i and S_j, $\vec{D}_{i,j} = -\vec{D}_{j,i}$, is called "DM vector" which results from the displacement of non magnetic ions located in the bisecting plane between $\overrightarrow{S_\iota}$ and $\overrightarrow{S_J}$ (see Fig.1). K is called coefficient of compass-type anisotropy ~~anisotropy~~. In the following we will suppose that tensor $\left|\vec{D}_{i,j}\right| = D$ independent of (i,j) for simplicity.

The last term in the Hamiltonian (1) is the energy of interface magnetoelectric interaction. We suppose that

$$H_{mf} = -\sum_{i,j,k} J_{ijk}^{mf} P_k^z \cdot \vec{S}_i \cdot \vec{S}_j \qquad (2)$$

In this expression J_{ijk}^{mf} is the interaction parameter between the electric polarization component $\vec{P}_j$ at the interface ferroelectric layer and its NN spins on the adjacent magnetic layer (See Fig. 1). Hereafter, for simplicity, we will assume that $J_{ijk}^{mf} = J^{mf}$ We note that this interface coupling can be assumed to be large, as it has been observed experimentally [35] where an experimental value of a magnetoelectric coupling constant is of the same order of magnitude as typical exchange interactions (even twice larger) in a multiferroic heterostructure (PMN-PT).

3. RESULTS AND DISCUSSION

A. GROUND STATE

Let us analyze the structure of the ground state (GS) in the case of multiferroic bilayer. We are interested in exploring the effect of competing frustrating interactions, so we fix $J_{i,j}^{m} = J^{m} = -1, J_{i,j}^{f} = J^{f} = 1$ as the scale through the rest of this work. In the antiferromagnetic layer on the triangular lattice, for the nearest neighbor antiferromagnet ($J^{mf} = D = 0$), in the absence of the external field the spins form a 120◦ spin-structure and a trivial sixfold degeneracy related to permutations of the spins on each site. In the case when we take into account DMI and magnetoelectric coupling between antiferromagnetic and ferroelectric layers it is more convenient using the numerical minimization method called “steepest descent method” to calculate and represent the ground state spin configuration. This method consists in minimizing the energy of each spin by aligning it parallel to the local field acting on it from its NN. We use a sample size N × N × L. For most calculations, we select N = 60-600 and L = 2 using the periodic boundary conditions in the xy plane. We investigated the following range of values for the interaction parameters J^{mf}

The ground state spin configuration in the case of competition of in-plane **D**, lattice frustration, compass-type anisotropy and magnetoelectric coupling has been studied by using steepest descent method with different values of J^{mf} and K. We note that the steepest descent method calculates the real ground state with the minimum energy to the value $D = -0.5$. For larger values, the angle between nearest neighbors tends to $\pi/2$ so that all magnetic exchange terms (scalar products) will lead to zero, the minimum energy corresponds to the DM energy. Small values of D and J^{mf} result in small values of angles between spins so that the GS configurations have noncollinear domains (not shown). Figure 2 shows the GS configurations of the magnetic interface layer for $D = -0.5, J^{mf} = -2.2$ in the absence of anisotropy.

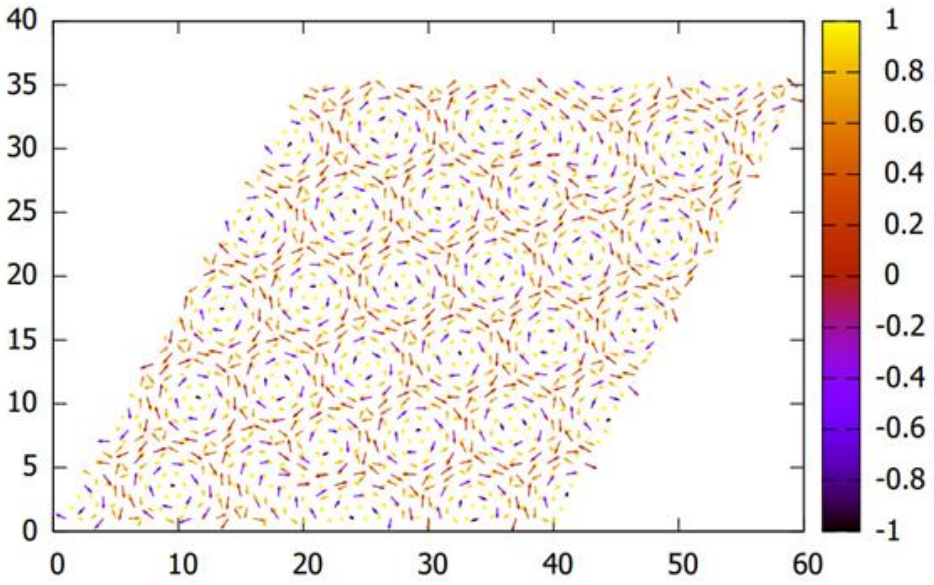

Fig. 2. GS configuration of the surface antiferromagnetic layer for $D = -0.5, J^{mf} = -2.2$ and $K = 0$. The right column shows the color distribution corresponding to the z-component of magnetization.

In Fig. 2 one observes an almost perfect lattice of skyrmions on a triangular lattice with a same diameter, we see that the central spin $S^z = -1$ in each skyrmion, and for spins in between the skyrmions $S^z = 1$. In the between, the xy components turn around the skyrmion center. A good periodicity of the skyrmion phase and perfect lattice structure is found here in the range of values case $J^{mf} \in (1.25, 3.5)$.

In Fig. 3, we show the stable ground states for different values of magnetoelectric coupling and anisotropy. A weak anisotropy ($K< 0.2$) renders a stable skyrmion lattice. A sufficiently large anisotropy ($K\geq 0.3$) suppresses the spin spiral, and the ground state becomes antiferromagnetic, as shown in the upper right corner of Fig. 3.

When $K\geq 0.3$ and magnetoelectric interaction $J^{mf} \in (2.0, 2.5)$ as shown on the lower right corner of Fig. 3, the ground state becomes a vortex. On the opposite limit of $K = 0$ and magnetoelectric interaction $J^{mf} \in (2.0, 2.5)$, the lower left corner of Fig. 3, the ground state is dominated by skyrmion lattices. At moderate values of anisotropy $K \in (0.0, 0.2)$ at the ground state skyrmions increase in diameter, the skyrmion lattice is destroyed, forming randomly distributed skyrmions, which are transformed into magnetic vortices.

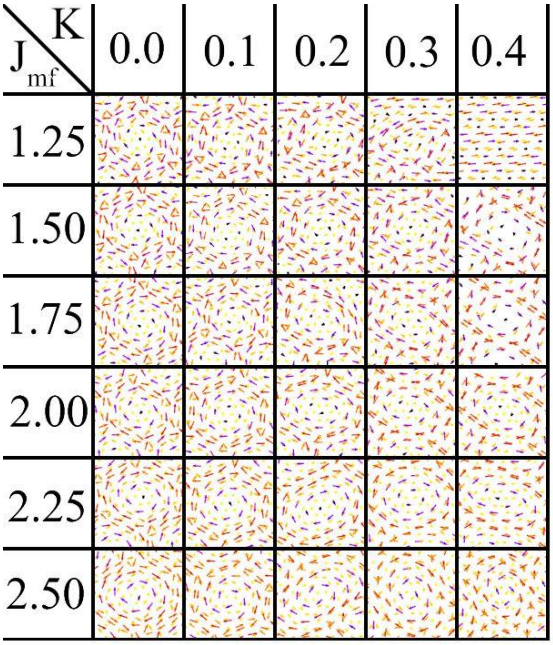

Fig. 3. Effect of anisotropy. The spatial profile of the z-component of the magnetization on a skyrmion. Each cell represents the ground state, obtained by using steepest descent method. Horizontal axis is the value of the anisotropy constant K; the vertical axis is interface magnetoelectric coupling. DMI and exchange parameters remain the same as in Fig. 2.

To understand the mechanism that enables a compass type magnetic anisotropy and magnetoelecric coupling to generate and stabilize skyrmion lattice phase, we must turn to the energies of the ground state.

The energy of different ground state as a function K for $J^{mf} = -2.2$ shown in Fig.4. When $K \in (0.0, 0.3)$ (blue area), the ground state energy increase with K. The skyrmion lattice state has the lowest energy as $D < 1.0$ mJ m^{-2}. As anisotropy K increases, a phase with randomly distributed skyrmions becomes the stable state (green ares), and it remains energetically more favorable (than skyrmion lattice state) even at D = 1.5 (not shown).

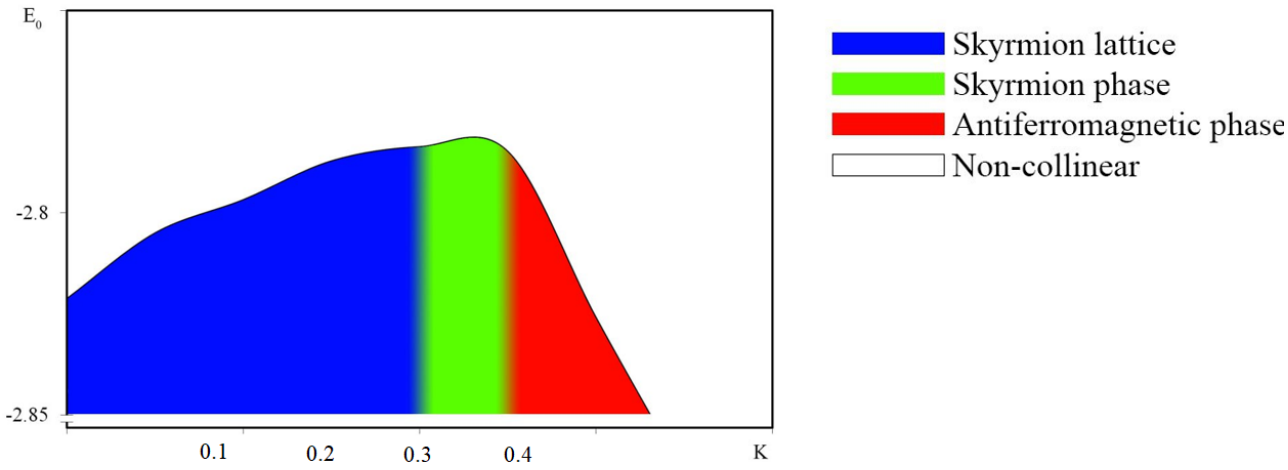

Fig. 4. The total energy as a function of the compass anisotropy for $J^{mf} = -2.2$ and $D = 0.5$.

As K increases above 0.4, the skyrmions are suppressed, and the antiferromagnetic state (red area) has the lowest energy even at large D. At K above 0.4 the ground state energy decreases with K.

B. MONTE CARLO RESULTS

We have used the Metropolis algorithm to observe the thermal fluctuations of the ground state spin configuration and to calculate physical quantities of the system at finite temperatures. It has been shown above that for D = 0.5, the skyrmion crystal phase exists for 2.0 < J^{mf} < 4.2 at zero T. In the case of in-plane **D** in a magnetoelectric bilayer for MC simulations we use a sample size $N \times N \times L$ with $N = 40 - 400$ and $L = 2$. Below, we study the phase transition of the skyrmion lattice phase shown above when we increase the temperature T. To see if the skyrmions and its lattice structure are stable at finite temperatures, we use MC simulations to calculate the averaged

energy per spin $\langle E\rangle$, the specific heat C_v and the order parameter Q. These quantities are defined as follows

$$\langle E\rangle = \frac{\langle H\rangle}{2N}, \qquad C_v = \frac{\langle E^2\rangle - \langle E\rangle^2}{k_B T^2}$$

$$Q(T) = \frac{1}{N(t_a - t_0)} \sum_i \left| \sum_{t=t_0}^{t_a} S_i(T,t) \cdot S_i(T=0) \right|$$

Where $\left|\sum_{t=t_0}^{t_a} S_i(T,t) \cdot S_i(T=0)\right|$ - the scalar product of spin at current temperature and the same spin at the ground state, which we have previously calculated using steepest descent method. These order parameters' temperature dependences for $J^{mf} = -1.75, J^{mf} = -2.0$ and $J^{mf} = -2.25$ are shown in Fig. 5(a). The energies of ferromagnetic subsystem versus T for the same values of J^{mf} are shown in Fig. 5(b).

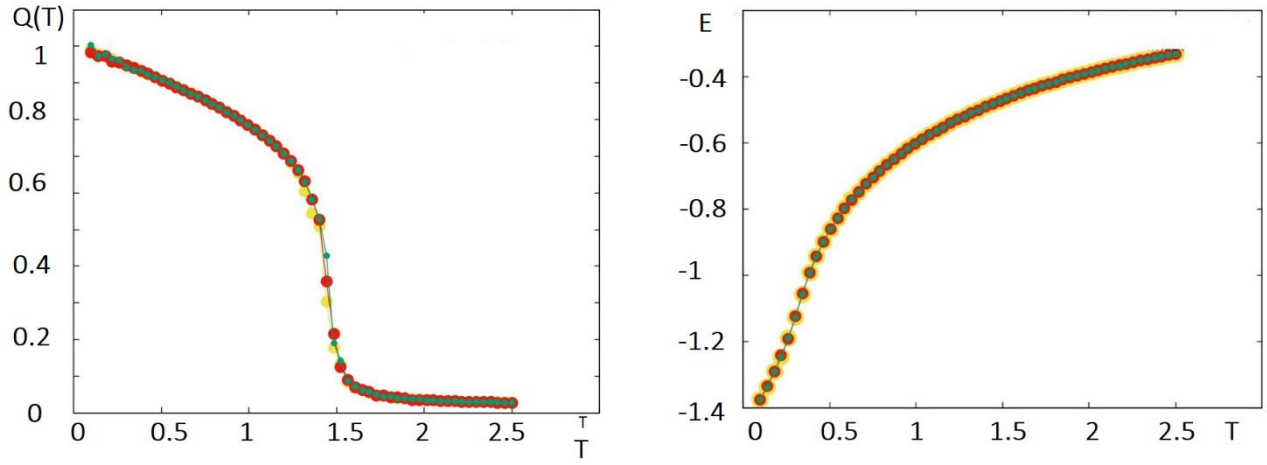

Fig. 5. a) Order parameter of antiferromagnetic layer versus T. b) Energy of antiferromagnetic layer versus T. The green, red and yellow dotted lines correspond to $J^{mf} = -1.75, J^{mf} = -2.0$ and $J^{mf} = -2.25$ respectively. Here $D = 0.5$, $K = 0$.

As the curves indicate, the antiferromagnetic layer undergoes a second order phase transitions at $T_C = 1.45\, J^m/k_B$ for $J^{mf} = (-1.75, 2.25)$. For the same set of parameters with non-zero anisotropy ($K = 0.3$) we obtain for the critical temperature $T_C = 1.99\, J^m/k_B$ (not shown).

In other words, the effect of anisotropy is reduced to a shift in the critical temperature without changing the type of phase transition. The results of Monte Carlo simulations allow us to conclude that the phase of the skyrmion lattice becomes more resistant to temperature fluctuations in the case of a highly anisotropic frustrated film.

4. CONCLUSIONS

In this paper, we have studied numerically using the steepest-descent method the magnetoelectric bilayer, composed of the non-frustrated ferroelectric film and the frustrated antiferromagnetic film. The latter is described by Heisenberg triangular lattice including a Dzyaloshinskii–Moriya interaction with an in-plane DM vector. We found that this system gives birth to a skyrmion lattice at T=0. We have studied the phase transition of this skyrmion crystal by using Monte Carlo simulations. Order parameter Q together with other physical quantities indicate that the skyrmion crystal is stable up to a rather high temperature. The effect of anisotropy is found to shift the critical temperature without changing the type of phase transition. The phase of the skyrmion lattice becomes more resistant and stable to temperature fluctuations in the case of a highly anisotropic frustrated film. This is very important because energy-efficient applications and devices based on skyrmions can operate only at finite temperatures.

REFERENCES

1. Khomskii D.I. (2006), Multiferroics: Different ways to combine magnetism and ferroelectricity, Journal of Magnetism and Magnetic Materials, Volume 306, Issue 1, 2006, Pages 1-8, https://doi.org/10.1016/j.jmmm.2006.01.238
2. Ramesh R. and Spaldin N.A. (2009), Multiferroics: progress and prospects in thin films, Nanoscience and Technology, pp. 20-28 (2009), https://doi.org/10.1142/9789814287005_0003
3. Mühlbauer S. et al., (2009) Skyrmion lattice in a chiral magnet. Science. 323, 5916, 915-919.

4. Nagaosa N. Tokura Y., (2013) Topological properties and dynamics of magnetic skyrmions, Nature Nanotechnology 8, 899-911, https://doi.org/10.1038/nnano.2013.243
5. Pyatakov A.P., Zvezdin A.K., (2013). Magnetoelectric and multiferroic media, PHYS-USP, 2012, 55 (6), 557–581, https://doi.org/10.3367/UFNe.0182.201206b.0593
6. Ge Y., Rothörl J., Brems M.A. et al, (2023) Constructing coarse-grained skyrmion potentials from experimental data with Iterative Boltzmann Inversion. Commun. Phys. 6, 30, https://doi.org/10.1038/s42005-023-01145-9
7. Scaramucci A., Shinaoka H., Mostovoy M.V., Müller M., Mudry C., Troyer M., and Spaldin N. A. (2018), Multiferroic Magnetic Spirals Induced by Random Magnetic Exchanges, Phys. Rev. X 8, 011005, Phys. Rev. X 8, 011005
8. Sampaio J., Cros V., Rohart S., Thiaville A., and Fert A., (2013) Nucleation, stability and current-induced motion of isolated magnetic skyrmions in nanostructures, Nature Nanotechnology, 8, 839 – 844, https://doi.org/10.1038/nnano.2013.210
9. Ghosh S., Manchon A., Železný J., (2022) Unconventional robust spin-transfer torque in noncollinear antiferromagnetic junctions, Physical Review Letters, 128, 9, 097702, https://doi.org/10.1103/PhysRevLett.128.097702
10. Hao X., Zhuo F., Manchon A., et al, (2021). Skyrmion battery effect via inhomogeneous magnetic anisotropy, Applied Physics Reviews, 8, 2, https://doi.org/10.1063/5.0035622.
11. Sharafullin, I. F., Kharrasov, M. K., Diep, H. T. (2019). Dzyaloshinskii-Moriya interaction in magnetoferroelectric superlattices: Spin waves and skyrmions. Physical Review B, 99, 21, 214420, https://doi.org/10.1103/PhysRevB.99.214420
12. Yadav A.K. et al., (2016), Observation of polar vortices in oxide superlattices, Nature volume 530, pages 198–201, https://doi.org/10.1038/nature16463

13. Paikaray B., Kuchibhotla M., Haldar A., Murapaka C., (2023). Skyrmion based majority logic gate by voltage controlled magnetic anisotropy in a nanomagnetic device, Nanotechnology, 34(22), 225202, DOI 10.1088/1361-6528/acbeb3
14. Perumal H. P., Sankaran Kunnath S., Priyanka B., Sinha, J. (2023). Tunable Conversion of Topological Spin Texture from Domain Wall Pair for Magnetic Memory Application in Specially Designed Magnetic Nanotracks. ACS Applied Electronic Materials, https://doi.org/10.1021/acsaelm.3c00391
15. Yu T., Luo Z., Bauer G. E. (2023). Chirality as generalized spin–orbit interaction in spintronics, Physics Reports, 1009, 1-115. https://doi.org/10.1016/j.physrep.2023.01.002
16. Staruch M., Li J.F., Wang Y., Viehland D. and Finke P., (2014), Giant magnetoelectric effect in nonlinear Metglas/PIN-PMN-PT multiferroic heterostructure, Appl. Phys. Lett. 105, 152902 (2014); https://doi.org/10.1063/1.4898039
17. Göbel B., Mertig I., & Tretiakov O. A. (2021). Beyond skyrmions: Review and perspectives of alternative magnetic quasiparticles, Physics Reports, 895, 1-28, https://doi.org/10.1016/j.physrep.2020.10.001
18. Yang S. H., Naaman R., Paltiel Y., et al. (2021). Chiral spintronics. Nature Reviews Physics, 3, 5, 328-343, https://doi.org/10.1038/s42254-021-00302-9.
19. Ramesh R., Schlom D. G. (2019). Creating emergent phenomena in oxide superlattices, Nature Reviews Materials, 4, 4, 257-268, https://doi.org/10.1038/s41578-019-0095-2
20. Tominaga J. et al. (2015), Giant multiferroic effects in topological GeTe-Sb2Te3 superlattices
21. Abid M., Ouahmane H., Lassri H., Khmou A. Krisnan R. J., (1999) Magn. Mater, 202, 335
22. Ortiz-Alvares H., Bedoya-Hincapie C., Restreppo-Parra E., (2014) Monte Carlo simulation of charge mediated magnetoelectricity in multiferroic bilayers, Physica B: Condenced Matter 454, 235-239

23. Bernand-Mantel A., Muratov C. B., Simon, T. M. (2020). Unraveling the role of dipolar versus Dzyaloshinskii-Moriya interactions in stabilizing compact magnetic skyrmions, Physical Review B, 101, 4, 045416. https://doi.org/10.1103/PhysRevB.101.045416
24. Wang L. et al, (2018) Ferroelectrically tunable magnetic skyrmions in ultrathin oxide heterostructures, Nature materials, 17, 12, 1087-1094, https://doi.org/10.1038/s41563-018-0204-4
25. Legrand W., Maccariello D., Ajejas F. et al., (2020) Room-temperature stabilization of antiferromagnetic skyrmions in synthetic antiferromagnets, Nat. Mater., 19, 34–42, https://doi.org/10.1038/s41563-019-0468-3
26. Shibata K., Iwasaki J., Kanazawa N. et al., (2015) Large anisotropic deformation of skyrmions in strained crystal, Nature Nanotech., 10, 589–592, https://doi.org/10.1038/nnano.2015.113
27. Koretsune T., Nagaosa N. Arita R. (2015) Control of Dzyaloshinskii-Moriya interaction in Mn1−xFexGe: a first-principles study. Sci Rep 5, 13302. https://doi.org/10.1038/srep13302
28. Wang J., Shi Y., Kamlah M., (2018), Uniaxial strain modulation of the skyrmion phase transition in ferromagnetic thin films, Phys. Rev. B 97, 024429, https://doi.org/10.1103/PhysRevB.97.024429
29. Magadeev E.B., Vakhitov R.M., Sharafullin I.F. (2022). Mechanism of Topology Change of Flat Magnetic Structures. Entropy, 24(8), 1104, https://doi.org/10.3390/e24081104
30. Liu L., Zhou C., Zhao, T. et al., (2022) Current-induced self-switching of perpendicular magnetization in CoPt single layer, Nat. Commun., 13, 3539. https://doi.org/10.1038/s41467-022-31167-w
31. Barker J., Tretiakov O. A. (2016). Static and dynamical properties of antiferromagnetic skyrmions in the presence of applied current and temperature. Physical review letters, 116(14), 147203. https://doi.org/10.1103/PhysRevLett.116.147203

32. Xia J., Zhang X., Tretiakov O. A., Diep H. T., et al., (2022) Bifurcation of a topological skyrmion string. Physical Review B, 105(21), 214402, https://doi.org/10.1103/PhysRevB.105.214402
33. Mohylna M., Gómez Albarracín F. A., Žukovič M., Rosales H. D., (2022), Spontaneous antiferromagnetic skyrmion/antiskyrmion lattice and spiral spin-liquid states in the frustrated triangular lattice, Phys. Rev. B., 106, 224406, https://doi.org/10.1103/PhysRevB.106.224406
34. Mohylna M., Žukovič M., (2022) Stability of skyrmion crystal phase in antiferromagnetic triangular lattice with DMI and single-ion anisotropy, Journal of Magnetism and Magnetic Materials, 546, 168840, https://doi.org/10.1016/j.jmmm.2021.168840
35. Usami T., Sanada Y., Shiratsuchi Y., Yamada S., Kanashima T., Nakatani R., Hamaya K. (2023). Converse magnetoelectric coupling coefficient greater than 10− 6 s/m in perpendicularly magnetized Co/Pd multilayers on Pb (Mg1/3Nb2/3) O3-PbTiO3, Journal of Magnetism and Magnetic Materials, 570, 170532, https://doi.org/10.1016/j.jmmm.2023.170532